

## Article

# Cyclic Behavior of Multiple Hardening Precast Concrete Shear Walls

Hongbo Jiang <sup>1,\*</sup>, Jian Sun <sup>2</sup>, Hongxing Qiu <sup>2</sup>, Dafu Cao <sup>1</sup>, Wenjie Ge <sup>1</sup>, Qiang Fang <sup>2</sup>, Hengwei Cui <sup>1</sup>  
and Kongyang Chen <sup>3</sup>

<sup>1</sup> College of Civil Science and Engineering, Yangzhou University, Yangzhou 225127, China

<sup>2</sup> Key Laboratory of Concrete and Prestressed Concrete Structures of Ministry of Education, Southeast University, Nanjing 211189, China

<sup>3</sup> Suzhou Electric Power Design Institute Co., Ltd., Suzhou 215011, China

\* Correspondence: jhb@yzu.edu.cn

**Abstract:** Precast Concrete (PC) shear walls are becoming popular in building structures. With “wet” connection techniques, PC shear walls often behave like conventional cast-in-place walls, where hardening occurs after yielding. In this study, two PC shear walls assembled by the “dry” connection technique, and one cast-in-place shear wall, were tested by means of quasi-static cyclic loading. The main purpose of the experiment was to systematically investigate the cyclic response of PC shear walls with varying types of vertical connection in the form of a friction-bearing device. The results showed that vertical bearing in devices, which mainly stems from the longitudinal elongation of PC wall panels, could enlarge the axial force of end column so that it provided an additional resistance moment. The PC shear wall with weak connection achieved ductile failure and second ascending branches on load-displacement relationship, i.e., secondary hardening, and the wall with strong vertical connection performed great moment capacity as well as tertiary hardening. Compared to cast-in-place walls, the peak load and cumulative hysteretic energy of PC shear walls increased by about 60% and 100%, respectively. A conceptual analysis of the multiple hardening phenomenon is presented based on experimental results.

**Keywords:** precast concrete; shear wall; longitudinal elongation; vertical connection; multiple hardening; conceptual analysis



**Citation:** Jiang, H.; Sun, J.; Qiu, H.; Cao, D.; Ge, W.; Fang, Q.; Cui, H.; Chen, K. Cyclic Behavior of Multiple Hardening Precast Concrete Shear Walls. *Buildings* **2022**, *12*, 2069. <https://doi.org/10.3390/buildings12122069>

Academic Editor: Mohamed K. Ismail

Received: 27 October 2022

Accepted: 22 November 2022

Published: 25 November 2022

**Publisher's Note:** MDPI stays neutral with regard to jurisdictional claims in published maps and institutional affiliations.



**Copyright:** © 2022 by the authors. Licensee MDPI, Basel, Switzerland. This article is an open access article distributed under the terms and conditions of the Creative Commons Attribution (CC BY) license (<https://creativecommons.org/licenses/by/4.0/>).

## 1. Introduction

In the past 20 years, developing countries such as China and Chile have made great progress. People flock to cities to live, and new constructions of middle- and high-rise building are constantly emerging. Reinforced Concrete (RC) shear walls, which provide strong, stiff, and cost effective lateral-load resisting members to resist earthquake load and wind load, have become the first choice in practical engineering [1]. In recent years, due to the rise in labor costs, construction quality requirements, and carbon emission problems, Precast Concrete (PC) construction has become a popular alternative to cast-in-place construction. The PC shear wall has attracted a lot of research in recent years, see Figure 1. With the development of building industrialization, PC construction can also be adopted in seismic regions [2]. Once proper connection is incorporated, one large shear wall can be disassembled into several well-sized PC wall members and then reassembled on site, so as to facilitate economical manufacture, transportation, and construction.

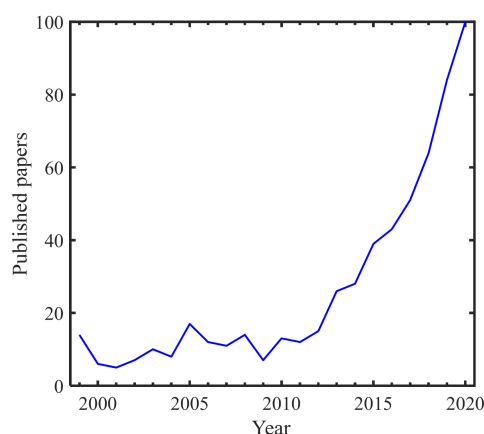


**Figure 1.** Numbers of published papers searched by “PC shear wall” in Web of Science database [3].

One issue about PC walls appears when connecting precast panels. Two kinds of connection are crucial to walls, namely horizontal connection and vertical connection, as shown in Figure 2. Most assembled construction techniques are based on “wet” methods [4–6], i.e., placing fresh concrete or cementitious grout after connecting steel bars with mechanical couplers/lap splices/welding [7,8]. As a consequence of labor-intensive construction methods, the “wet” method has lagged behind the efficiency demands of building industrialization. To avoid these drawbacks, some researchers combined the connection technique with the “dry” method, such as steel shear key [9], damper [10,11], buckling restrained plates [12], and damping devices at the toes of the wall [13]. However, site-welding operations are required for the assembly of wall panels with these convenient equipment, which bring other potentially dangerous and harmful factors, pointing to the bolt-based assembly method as a more attractive alternative. Another issue is design philosophy. Along with cast-in-place work in joints, a simplified process is to design the PC members as a cast-in-place one. Hence, the characteristics of cast-in-place members (such as accumulated damage, low ductility, and low resilience) are also retained [14,15]. The lateral load–top displacement relationship is often used to assess the seismic behavior of a shear wall, see Figure 3. Generally, most slender shear walls experience the elasticity, hardening, and softening phase. In particular, after flexural yielding, different walls may fail in different ways, including fracture/buckle of longitudinal reinforcing bars, crushing of the boundary element zone, and concrete crushing in the web [16]. With proper horizontal and vertical connection, PC technology provides a chance to delay the degeneration process and improve the ductility.

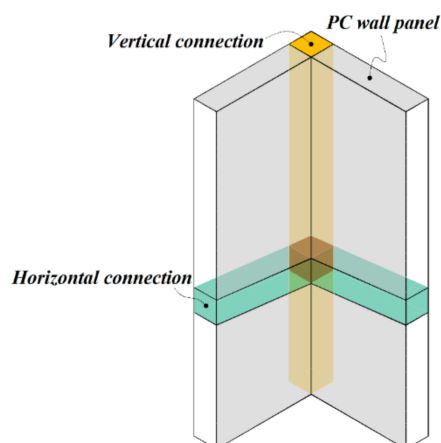


**Figure 2.** Horizontal and vertical connection in PC wall system.

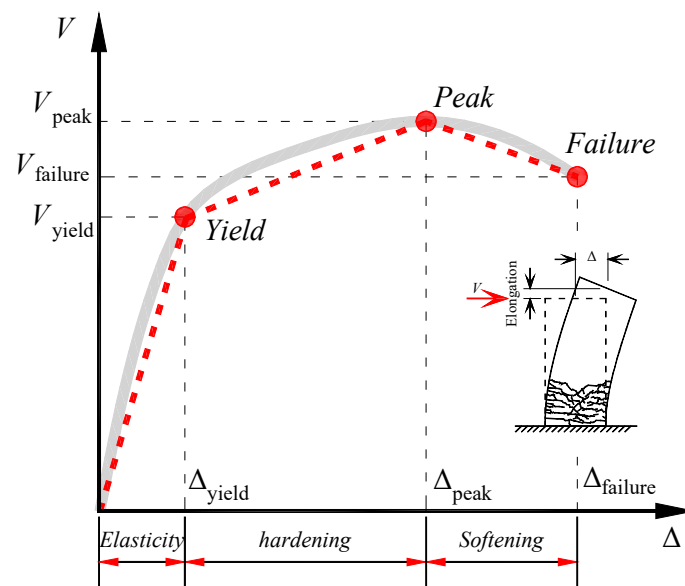


**Figure 3.** Lateral load–top displacement relationship (grey solid line) and classic backbone (red circle markers and dashed line) of cast-in-place shear wall.

As a common damage phenomenon depicted in Figure 3, the axial elongation is generally considered to be caused by accumulated damage in the plastic hinge zone [17–20]. Axial elongation, elongation of tensile side, and elongation of compressive side are collectively called “longitudinal elongation” here. In ductile RC shear walls, the longitudinal elongation grows quickly after the plastic hinge is formed at the bottom of the wall [21,22], which provides insight for a new connecting philosophy and innovative working mechanism for PC walls. Limited existing research could be retrieved on the elongation of RC shear walls [18,23–25], not to mention the effective utilization of this kind of deformation. Recently, a bolt-based PC shear wall was developed and experimentally validated to take into account the wall elongation [22]. Figure 4 depicts the schematics of the proposed PC shear wall system, in which steel square columns representing the end column and friction-bearing devices with limited slippage are placed. As expected, the longitudinal elongation could cause the slipping of friction-bearing devices during cyclic loading. The advantage of the new system is great moment capacity and ductility, however, in the early study [22], the walls failed with concrete spalling around the devices at the end of test.

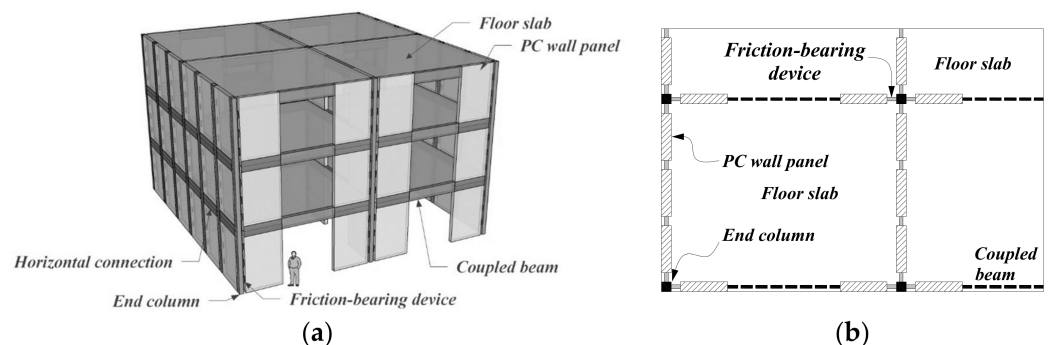


**Figure 4.** Proposed PC shear wall system [22]. (a) 3D view; (b) Plan view.

To better understand the behaviour of the new-type PC shear wall, this paper describes an experimental investigation and discussion of PC shear walls. Different from the previous experimental study [22], a rigid column base and various vertical connections were adopted, see Figure 5. Rigid column base is much more common in engineering practice and can be considered to enhance the stability and moment resistance of the column. Experimental results of walls with weak or strong vertical connection tested to failure are reported in

terms of multiple hardening phenomena. As well as the secondary hardening observed in the previous study, a new tertiary hardening was presented and contrasted herein. A discussion is provided to explain these uncommon phenomena.

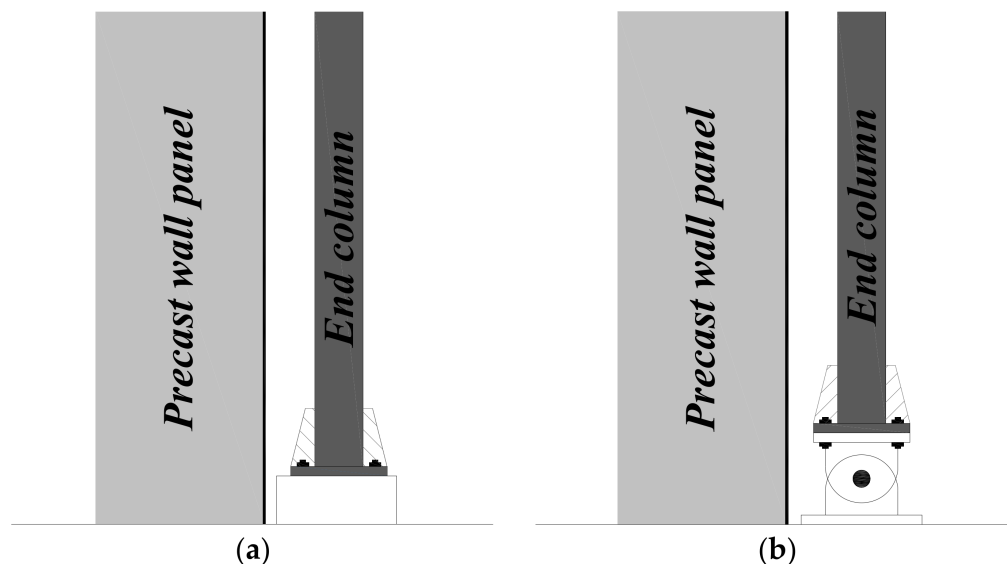


**Figure 5.** Comparison of column base between current and previous test. (a) Column base of testing wall in this paper; (b) Column base of previous wall [22].

## 2. Experimental Program

The testing walls are reported in this section, together with the loading scheme.

### 2.1. Testing Walls

Three testing walls, named W0 (cast-in-place construction), W1-R, and W2-R (precast construction) were designed and built for quasi-static reversed cyclic loading tests. As depicted in Figures 4 and 6, the testing PC shear walls are basic members extracted from the overall PC system, with a loading beam and a short wall segment cast at the top of wall panel and foundation block, respectively. As control variables, the cast-in-place wall and wall panels were designed in same section dimensions and reinforcement details. The wall panels were measured  $2250 \times 1000 \times 120$  mm (i.e., aspect ratio = 2.25) and reinforced with three diameters of steel bars.

Similar to the previous proof-of-concept test [22], the wall panel is designed as a 1/2-scale RC shear wall with boundary elements on the left and right side in accordance with Chinese standard GB 50010-2010 [26]. To facilitate the assembly of the horizontal connection, steel shoes were placed at the bottom end of the wall panel before casting, with vertical steel bars being welded on the inner surface of the steel shoe. To facilitate assembly of the vertical connection, two kinds of vertical connection were utilized for the PC shear walls. W1-R was cast with built-in bolts at both sides of the wall panel, resulting in a weak vertical connection; a thicker friction-bearing device and vertical steel shoes were utilized in W2-R, resulting in a strong vertical connection. The details of the horizontal and vertical connections are depicted and summarized in Figures 7 and 8, and Table 1. Two PC shear walls were designed with comparable limited slippage (12 mm) and varying magnitude of friction in the devices. As emphasized before, different from the previous experimental study [22], which contained a pin base under the end column, this time the PC shear walls contained a rigid column base, see Figure 5.

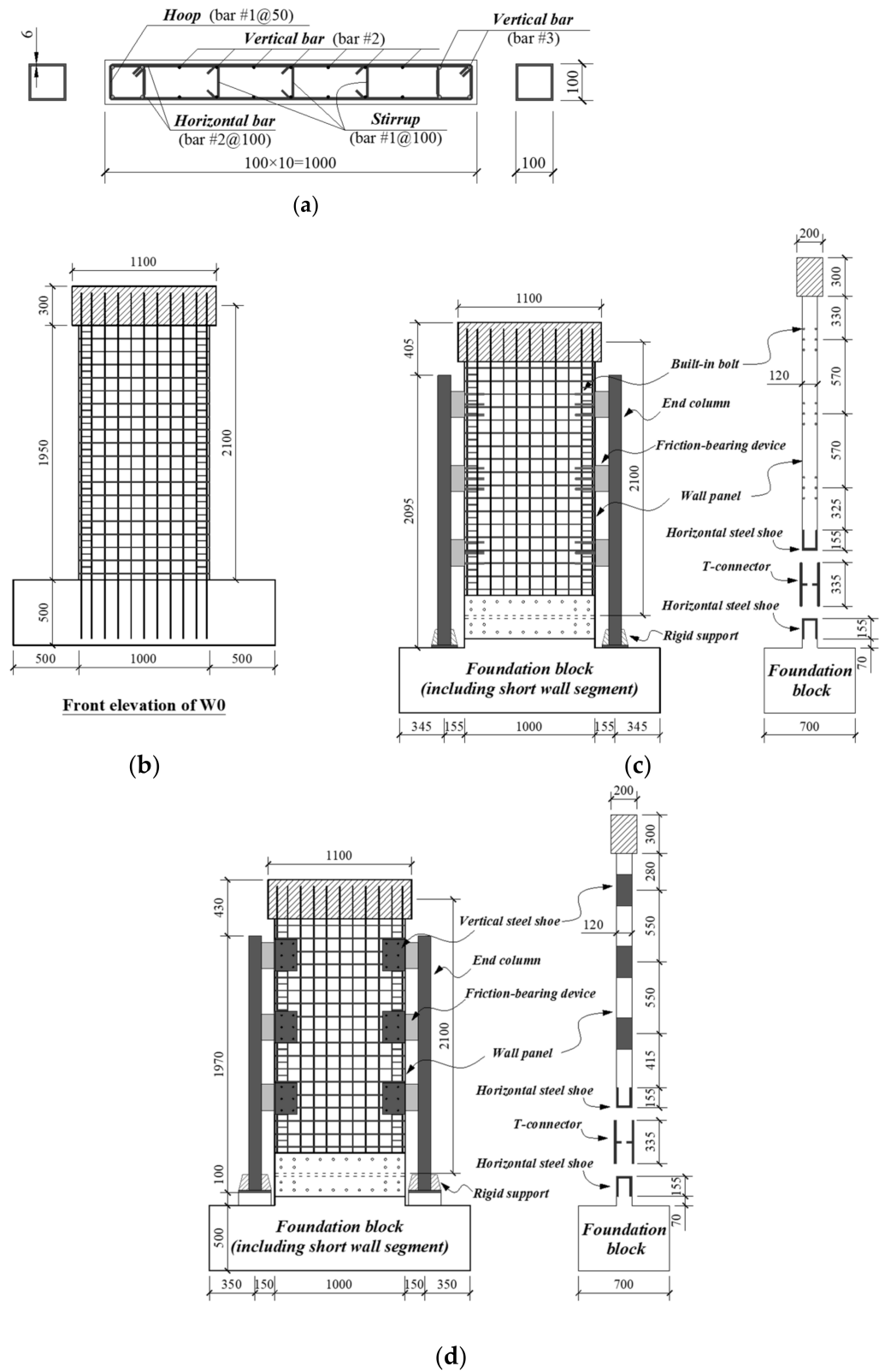


Figure 6. Details of walls (unit: mm). (a) Cross section of PC shear wall; (b) W0; (c) W1-R; (d) W2-R.

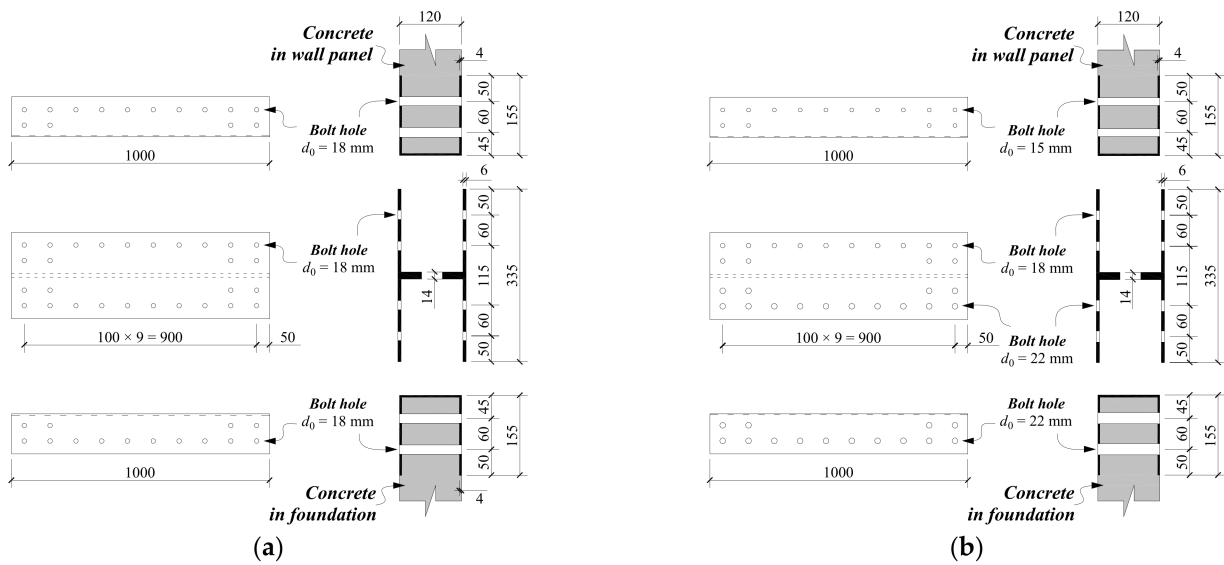


Figure 7. Details of horizontal connection in PC walls (unit: mm). (a) W1-R; (b) W2-R.

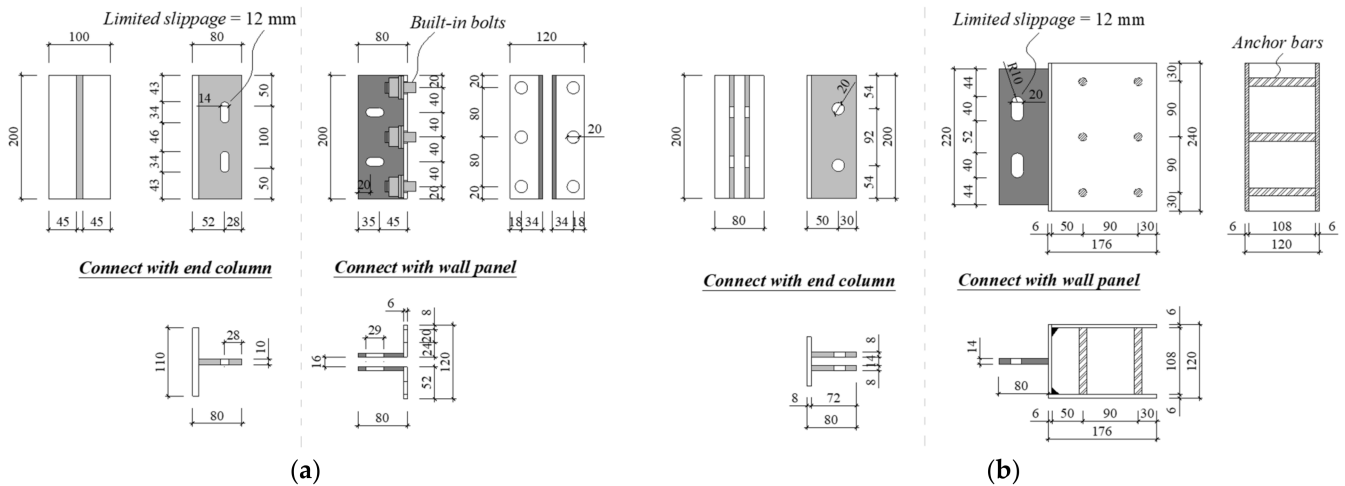


Figure 8. Details of vertical connection in PC walls (unit: mm). (a) W1-R; (b) W2-R.

Table 1. Details of vertical connection.

Testing PC Walls	Column Base	Friction-Bearing Device		
		High Strength Bolt	Friction Applied by One Bolt	Friction Applied by One Device
W1-R	Rigid	M12	11.4 kN	22.8 kN
W2-R	Rigid	M18	20.0 kN	40.0 kN

During the member casting, standard concrete cubes (150 × 150 × 150 mm) and prismoids (150 × 150 × 300 mm) were cast according to Chinese standard GB/T 50081-2002 [27]. Steel coupons for types of steel bar and steel plate were also prepared and tested in accordance with GB/T 228.1-2010 [28]. W0 and W1-R were cast in one batch with measured concrete compressive strength  $f_c = 27.0$  MPa, and for W2-R another batch measured at  $f_c = 27.5$  MPa. Testing results of steel are summarized in Table 2.

### 2.2. Loading Scheme

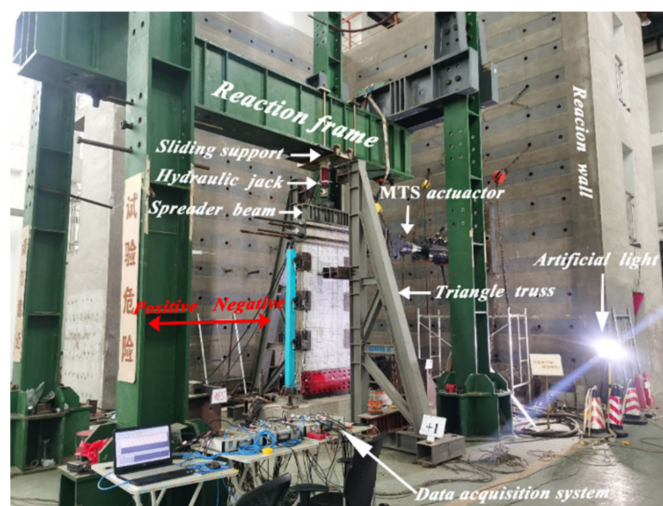
Three walls were tested by a horizontal reversed quasi-static cyclic loading and constant axial force  $P$ . The axial force and horizontal load were both applied on the loading beam, the former by a hydraulic jack and the latter by an MTS actuator. A sliding support was seated between the reaction frame and hydraulic jack so that both vertical and

horizontal load could be applied simultaneously. The axial load applied on W0 and W1-R was 235 kN, and on W2-R it was 220 kN. The corresponding axial load ratio,  $P/f_c A_g$ , for the above two axial loads were 0.073 and 0.067, respectively, where  $A_g$  is gross area of the concrete section. The light axial load was chosen for two reasons, being that heavy axial load may restrain the elongation, and safety considerations for an innovative wall test. The foundation block and a pair of out-of-place triangle trusses were fixed to the strong floor to provide a stable testing boundary. Typical testing photo is illustrated in Figure 9a.

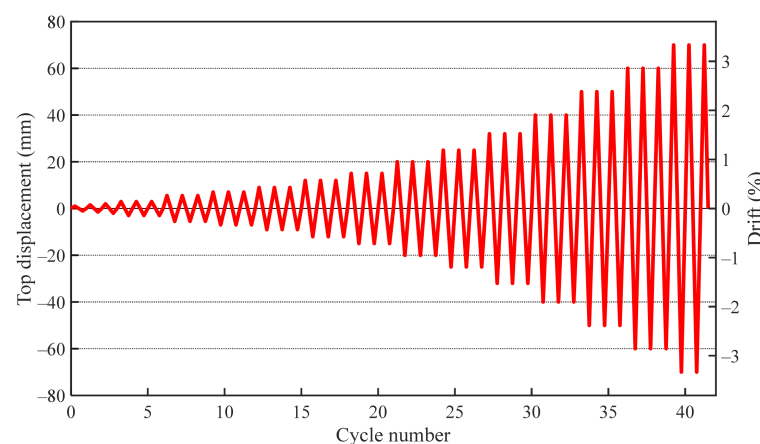
**Table 2.** Testing results of steel properties.

Material	Diameter/Thickness (mm)	Yield Strength (MPa)	Ultimate Strength (MPa)
Bar #1	6.7 (6.5)	370.9 (314.4)	523.0 (527.5)
Bar #2	8.0 (8.0)	338.8 (308.1)	509.4 (488.1)
Bar #3	9.5 (8.0)	490.0 (308.1)	544.3 (488.1)
Plate	6.0 (6.0)	372.0 (337.1)	431.8 (380.5)

Note: The data out of brackets are properties of W0 and W1-R. The data in brackets are properties of W2-R.



(a)



(b)

**Figure 9.** Testing setup and loading protocol. (a) Photo of W2-R; (b) Loading protocol.

The displacement-controlled protocol of horizontal load is described in Figure 9b, with one cycle per step before 2.0 mm top displacement, and after that, three cycles per step until failure [22]. The failure is defined as the recovery force degrading to less than 85% of the peak lateral load, as generally adopted in seismic tests [29,30]. Additionally, the drift ratio was stated as  $\Delta/H_e$ , where  $\Delta$  is the top displacement (i.e., horizontal displacement

at the lateral loading point), and  $H_e$  is the effective height 2100 mm shown in Figure 6. Apart from the top displacement and lateral load measured by the sensors in the actuator, displacement gauges were placed at the foundation block and friction-bearing devices to monitor the potential slippage. Numbers of strain gauges were mounted on the steel bars and end columns to measure the real-time steel strain. Detailed locations of gauges are reported in Figure 10.

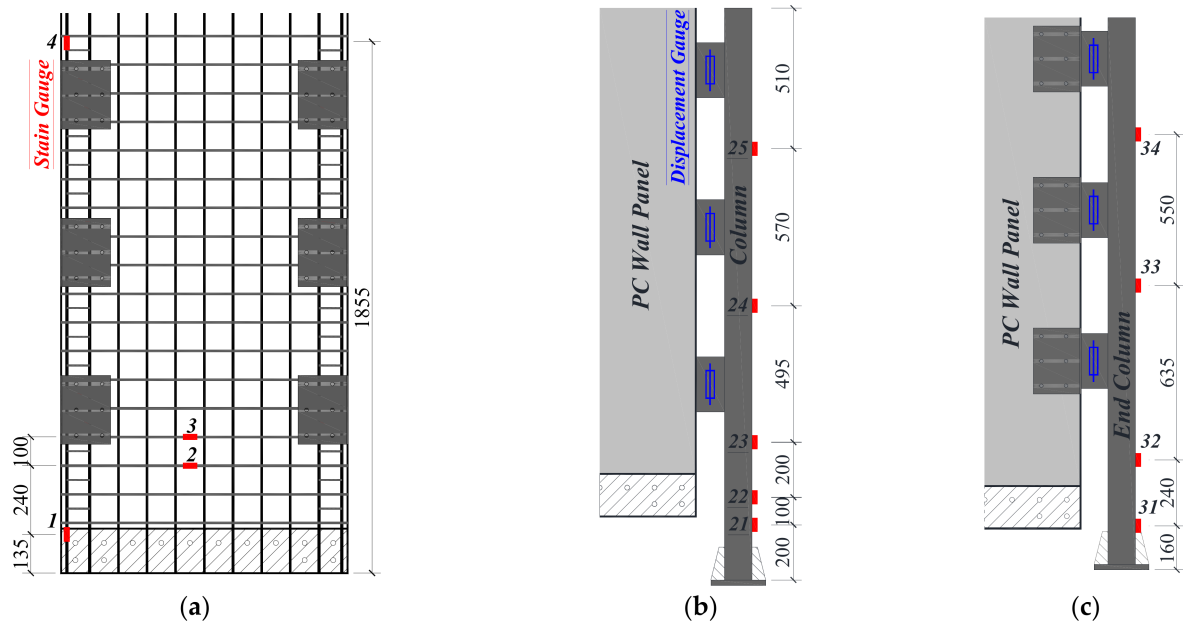


**Figure 10.** Instrumentation of wall. (a) Gauges mounted on wall; (b) Gauges mounted on W1-R end column; (c) Gauges mounted on W2-R end column.

### 3. Experimental Results

The response pertaining to friction-bearing devices, damage, and failure modes, load–displacement relationship, measured strains, stiffness reduction, and energy dissipation are reported in this section.

#### 3.1. Working Mechanism and Response of Friction-Bearing Devices

See Figures 11 and 12, “vertical bearing” (i.e., the bolt bearing in the friction-bearing devices) may occur during the cyclic loading, which stems from the magnitude of limited slippage. Both PC shear walls were designed with same limited slippage, 12 mm. The vertical slippage in devices was recorded by displacement gauges, whose responses are shown in Figure 13.

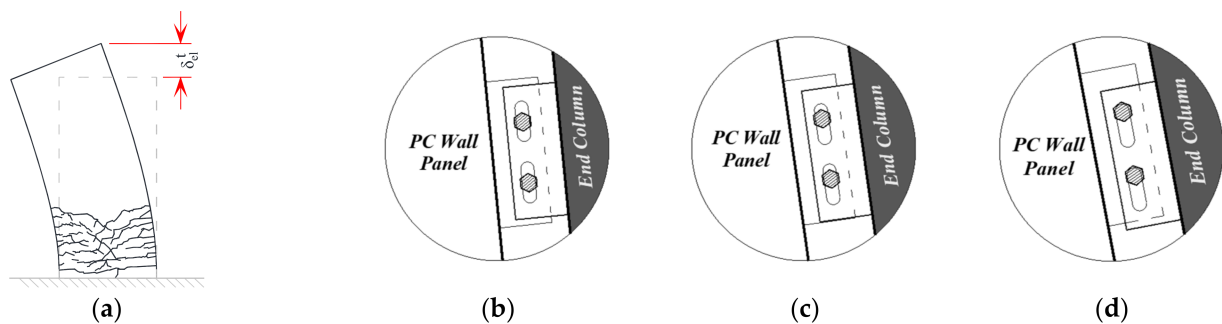


**Figure 11.** Vertical bearing of Tensile side (VT). (a) Longitudinal elongation of tensile side; (b) Before slip; (c) Slipping; (d) Bolt bearing.

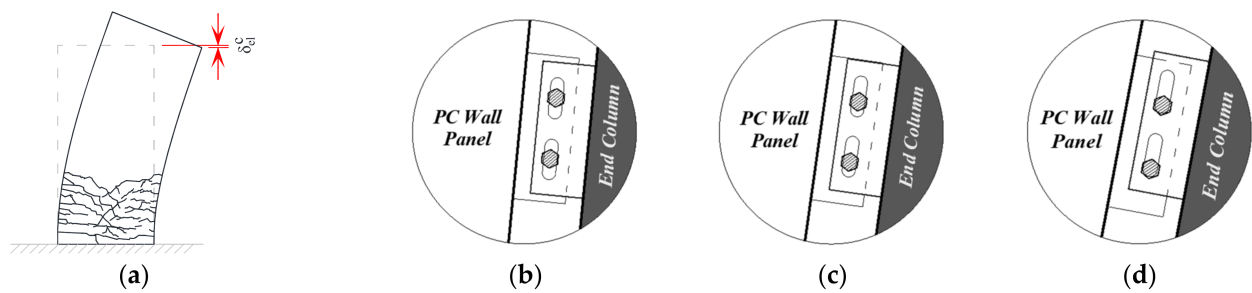


**Figure 12.** Vertical bearing of Compressive side (VC). (a) Longitudinal elongation of compressive side; (b) Before slip; (c) Slipping; (d) Bolt bearing.

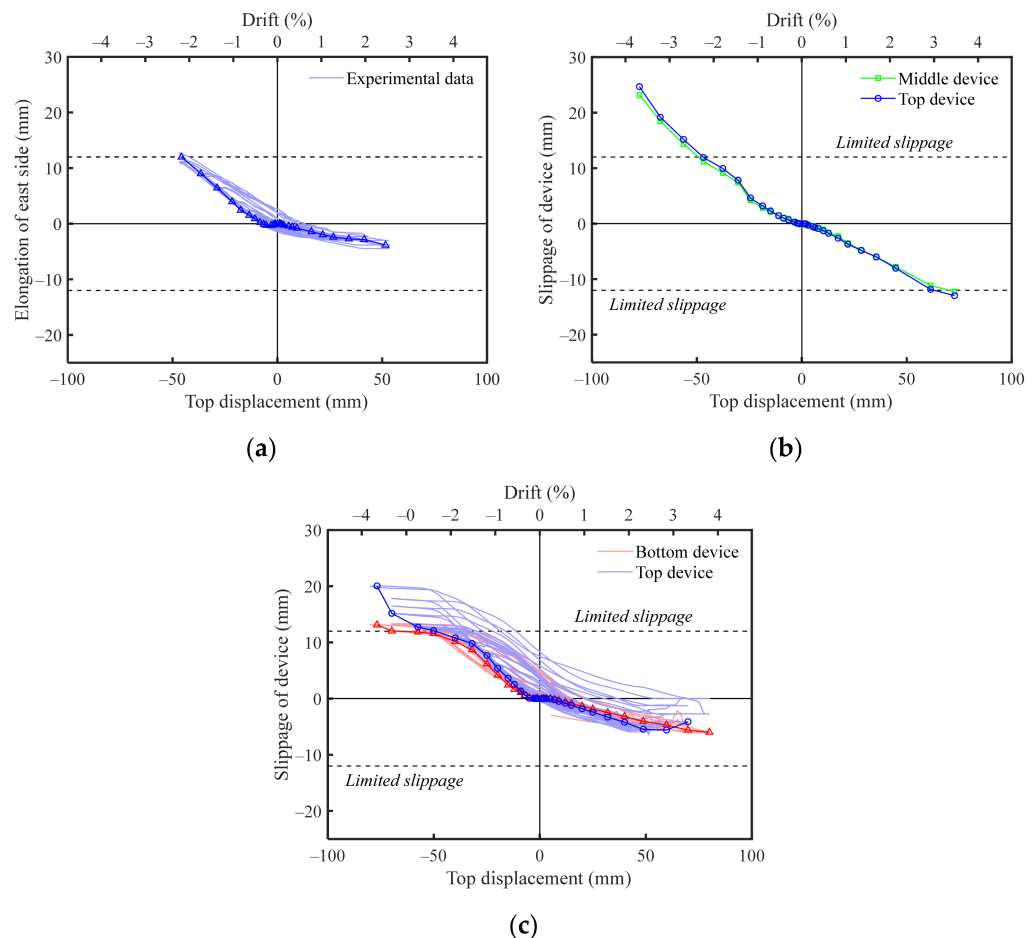


**Figure 13.** Results of vertical slippage and elongation. (a) Elongation in W0; (b) Vertical slippage in W1-R; (c) Vertical slippage in W2-R.

Table 3 summarizes the lateral top displacements when vertical bearing occurred, and two PC shear walls behaved similarly. Wall W1-R and W2-R attained “Vertical bearing of Tensile side” (“VT” for short) at a drift ratio of 1.33% (top displacement 28 mm) and 1.48% (top displacement 31 mm), respectively. The rough value of lateral top displacement when VC occurred reached an approximate drift ratio of 3.05% (top displacement 64 mm) for W1-R and 2.86% (top displacement 60 mm) for W2-R. The occurrence time of vertical bearing was comparable to the previous study [22], which indicated that the pin/rigid column base had relatively small influence on the working mechanism of vertical bearing. Because the slipping response for all three walls were comparable, the friction in devices was considered to have no significant influence on the elongational phenomenon. It can be inferred the effect of friction on the left and right sides balances itself out.

**Table 3.** Top displacement when “vertical bearing” occurred.

Test Walls	“Vertical Bearing of Tensile Side”		“Vertical Bearing of Compressive Side”	
	Positive (mm)	Negative (mm)	Positive (mm)	Negative (mm)
W1-R	28	32	64	64
W2-R	31	30	60	60

Another interesting and important behavior is that, once VT occurred, strong vertical connection (W2-R) almost stopped the device from slipping, while weak vertical connection (W1-R) did not. The continuous increase in slippage in W1-R is due to the low robustness of weak friction-bearing devices. Furthermore, the slippage of the top device in W2-R increased again when the top displacement was over 60 mm, resulting from the severe damage of the upper wall part.

### 3.2. Damage and Failure Mode

Early in the loading, all three walls behaved in a comparable manner, with flexural cracks initially opening above the horizontal connection as the 0.10% drift ratio for wall W0 and 0.24% drift ratio for other two PC shear walls, with later cracks gradually extending diagonally downwards. Before the occurrence of vertical bearing (20 mm, 0.95% drift ratio), we found less diagonal and X-shaped cracks in the two PC shear walls, similar to previous PC walls using pins as the column base [22], demonstrating that bending deformation was the major factor in PC wall panels compared with cast-in-place walls. Furthermore, the less cracks also mean that shear force demand in the PC walls was observably decreased by vertical connection in the initial loading period.

After these initial cracks appeared, no more cracks were found in W0. However, the PC shear walls continued to crack along with vertical bearing. VT occurred during the load step to 1.52% drift ratio (top displacement 32 mm), together with the diagonally oriented cracks around friction-bearing devices.

Finally, three walls failed in different ways, as depicted in Figure 14. W0 failed in flexure-shear mixed mode, with X-shape cracks from the bottom end to the top, and concrete crushing at the wall toes at the end. Additionally, VC occurred together with distinguishing failure in two PC shear walls. For PC shear wall W1-R, which assembled with weak vertical connection, concrete spalling and crushing were observed around the friction-bearing devices as well as the toes of the wall panels. For PC shear wall W2-R, being equipped with strong vertical connection prevented the crushing failure around the vertical connections, but the wall failed with diagonal tension cracking and concrete crushing in the upper wall part. Figure 15 shows the cracking observation of all three walls after testing.

The failure mode of wall W2-R is unusual but understandable. See Figure 16, the six devices divide the wall panel into four wall parts: upper, middle 1, middle 2, and bottom. The VT and VC of strong vertical connection restrained the elongation of the wall panels strictly, leading to high additional axial load in the middle and bottom wall parts. This constraint further increased the flexural and shear capacities of the middle and bottom wall parts, followed by the slow deterioration of the bottom plastic hinge region, and the bottom of wall panel ceased cracking, see Figure 14e,f. The upper wall part became a nominal “squat wall” and experienced shear failure.

### 3.3. Lateral Load–Top Displacement Relationship

The measured lateral load versus top displacement relationships of three walls are drawn in Figure 17a–c, and the comparison of backbone curves is reported in Figure 17d. The lateral top displacement when VT and VC occurred are marked with the black and red dotted lines, respectively. The hysteretic loops of W1-R and W2-R are fatter than those of W0 with incremental lateral top displacement. Furthermore, the vertical connection and accessory friction failed to rise the residual displacements associated with the cyclic loading.

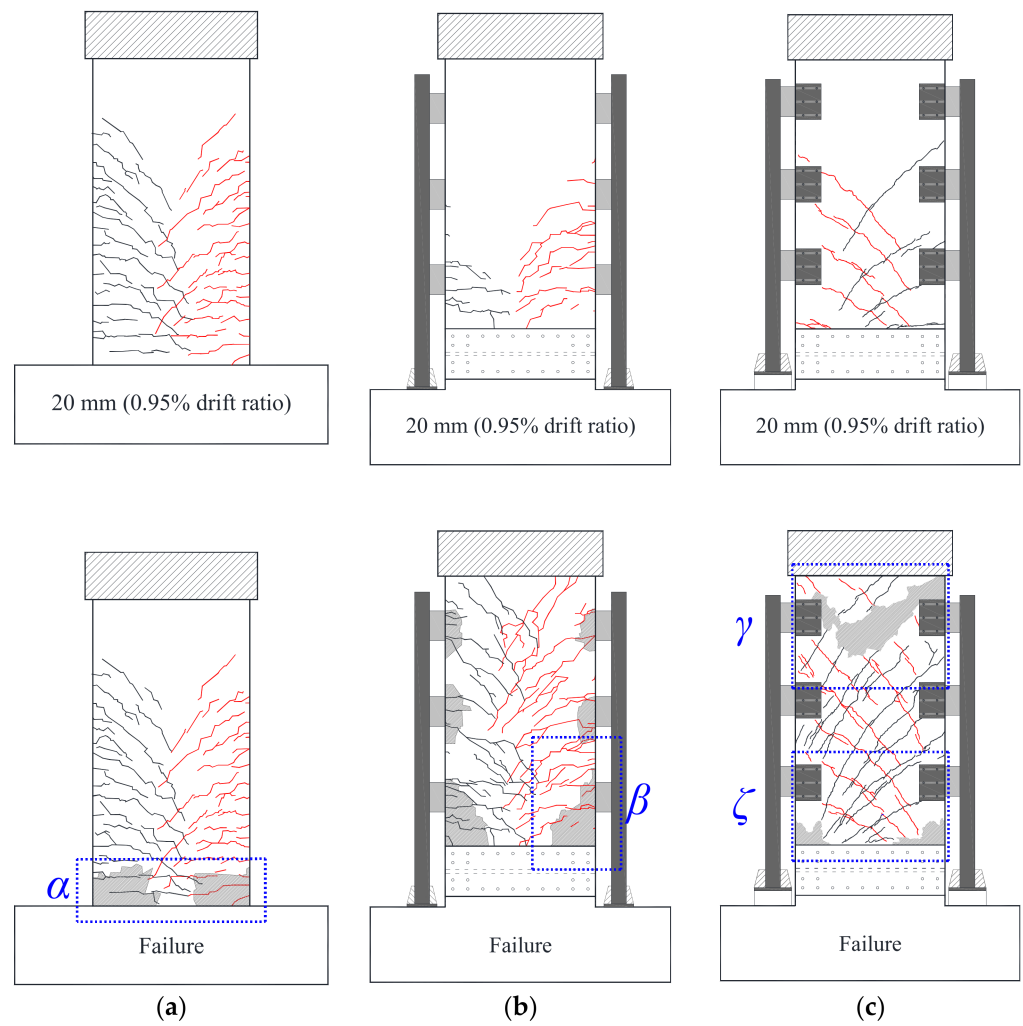


**Figure 14.** Crack distribution of testing walls (black and red lines represent the cracks as subjected to different loading direction). (a) W0; (b) W1-R; (c) W2-R.

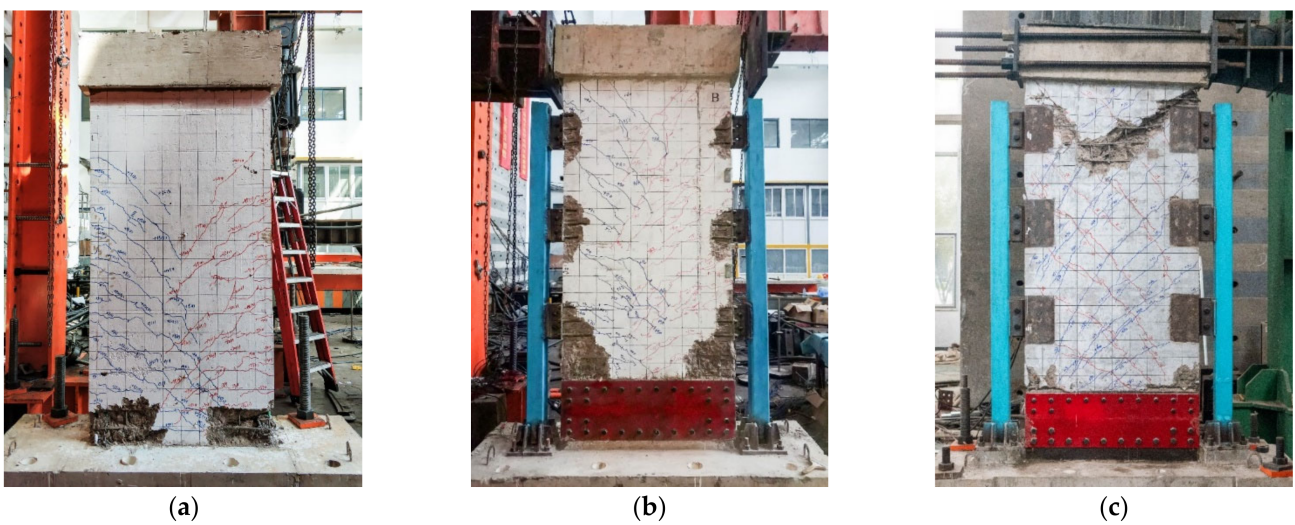


**Figure 15.** Cont.

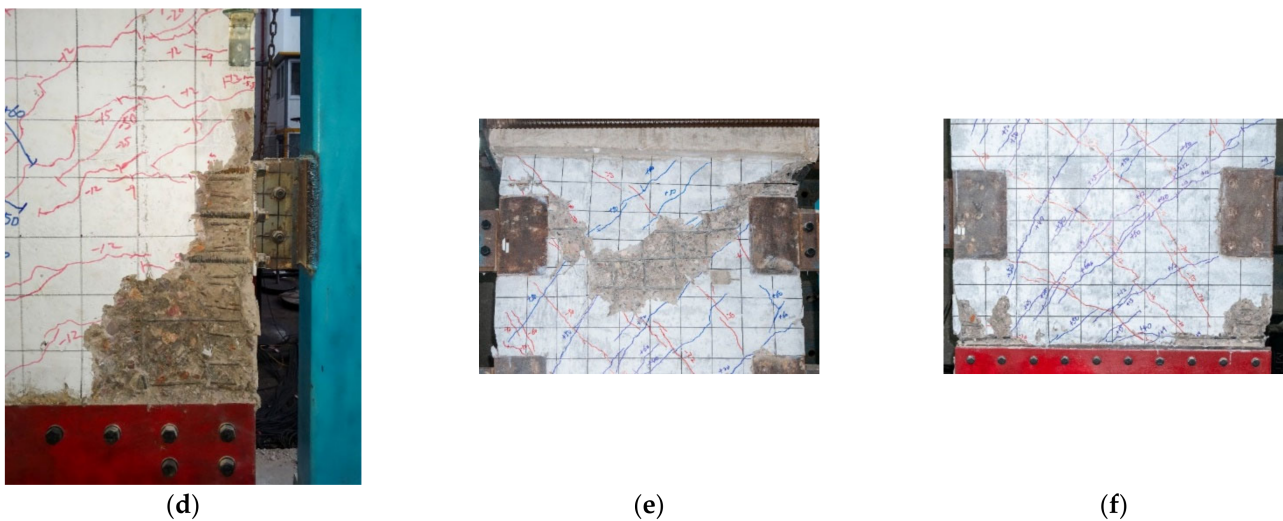


**Figure 15.** Cracking observation after test (blue and red lines represent the cracks as subjected to different loading direction). (a) Global damage in W0; (b) Global damage in W1-R; (c) Global damage in W2-R; (d) Local damage in W1-R (detail from zone  $\beta$ , Figure 14d); (e) Local damage at the top of W2-R (detail from zone  $\gamma$ , Figure 14f); (f) Local damage at the bottom of W2-R (detail from zone  $\zeta$ , Figure 14f).

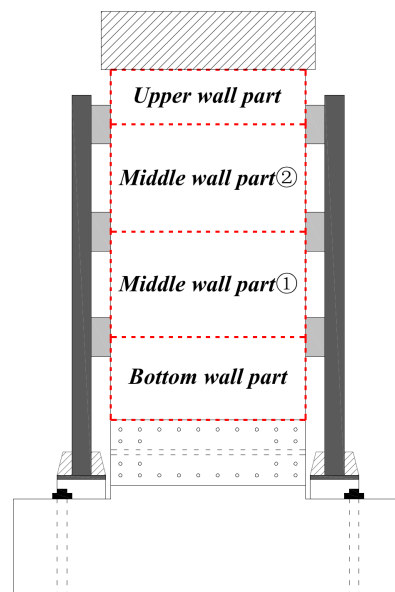


**Figure 16.** Wall parts divided by friction-bearing devices in PC shear wall.

Four key points representing the behavioral phases were identified in Figure 17. The same as the definition of failure in the preceding part of the paper, the ultimate point was defined as 85% peak lateral load of response [29,30]. The cast-in-place wall W0 achieved peak lateral load at a drift ratio of 1.03% with 203.2 kN. Both PC shear walls achieved great moment capacity and drift capacity (i.e., drift ratio of ultimate point). W1-R and W2-R achieved peak loads at a drift ratio of 2.92% (315.1 kN) and 3.81% (365.1 kN), respectively. The peak loads of PC shear walls increased by about 60% when compared to cast-in-place W0. Compared with wall W1-R, the peak lateral loads of wall W2-R with strong vertical connection increased by 16% (Positive direction), and top displacement of ultimate point decreased by 9% (Positive direction). Wall W1-R was more ductile than wall W2-R, which was in accordance with the response characteristics about peak lateral loads and top displacement. In fact, the weak vertical connection could be considered to be a kind of ductile connection to some extent, although it failed it resulted in wall W1-R being more

ductile without sudden load loss. For safety reasons, wall W2-R, in which the upper wall part failed in shear, was not tested to 85% peak load in positive direction.

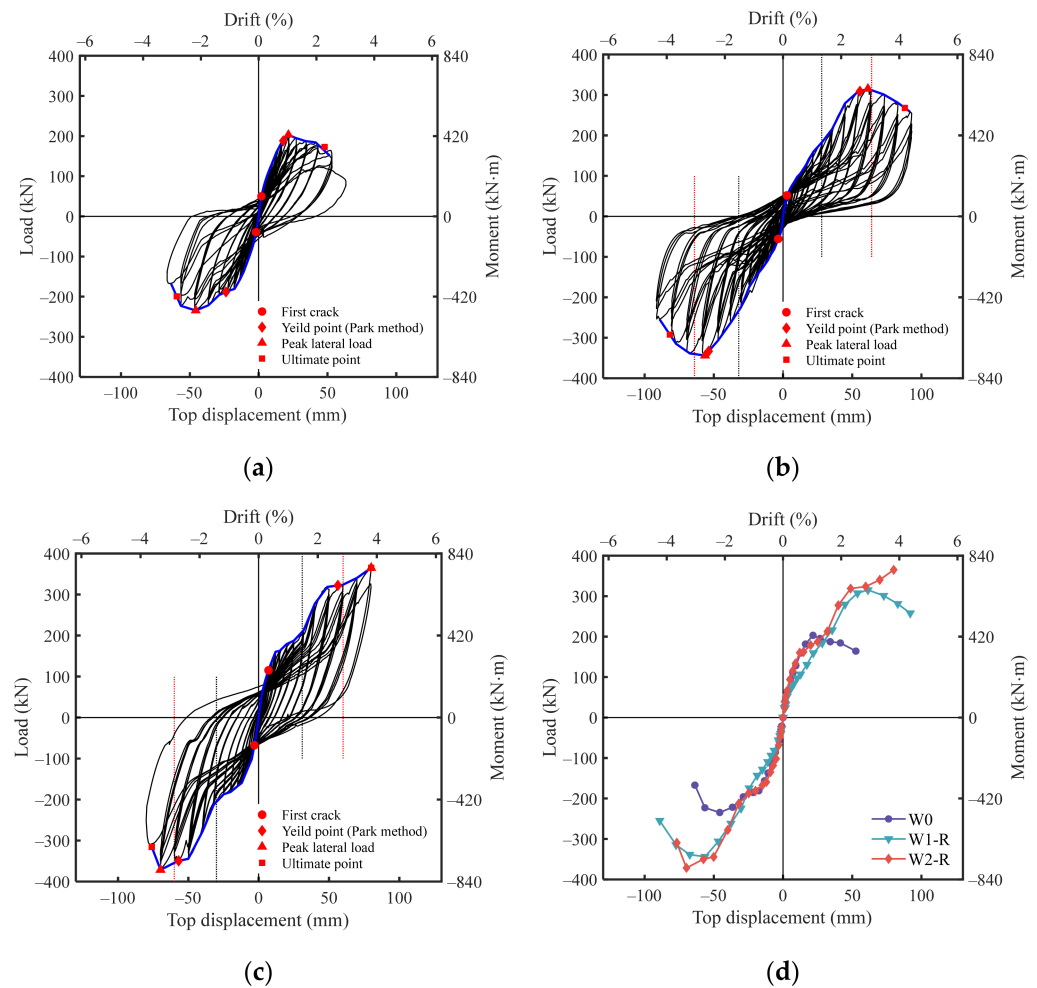


**Figure 17.** Measured lateral load–top displacement responses (black dotted lines represent VT, red dotted lines represent VC). (a) W0; (b) W1-R; (c) W2-R; (d) Comparison of backbone curves.

VT could be able to provide additional resistant moment, the wall W1-R and W2-R here reproved the fact and further demonstrated the influence of weak/strong connection. For wall W1-R, VT enlarged the internal force of the vertical connection, concrete around the built-in bolts cracked gradually, then, VC which led to upward compression in devices meantime widened the existing cracks. Eventually, W1-R reached its peak lateral load. As can be observed in Figure 17, the second ascending branches were governed by VT and peaked when VC occurred. For wall W2-R, both VT and VC increased, which caused the overall response to be extra ascending branches, however, due to hardening of the middle and bottom wall parts influenced by VC, the upper wall part failed finally. In this special way, it is interesting to note that W1-R achieved secondary hardening, while W2-R achieved tertiary hardening.

### 3.4. Measured Strain

The strain of vertical bars above the horizontal connection is crucial data to estimate the working phases of shear wall. The measured strains in vertical bars are depicted in Figure 18. With well welding between vertical bars and steel shoes, the bars of all walls yielded at a comparable top displacement, approximately 20 mm (0.95% drift ratio). Apparently the hysteretic loops of W1-R and W2-R are slimmer than those of W0. It can be

inferred that, before the occurrence of vertical bearing, the vertical connection dissipated most of the energy, while the PC wall panel itself only dissipated a small part.

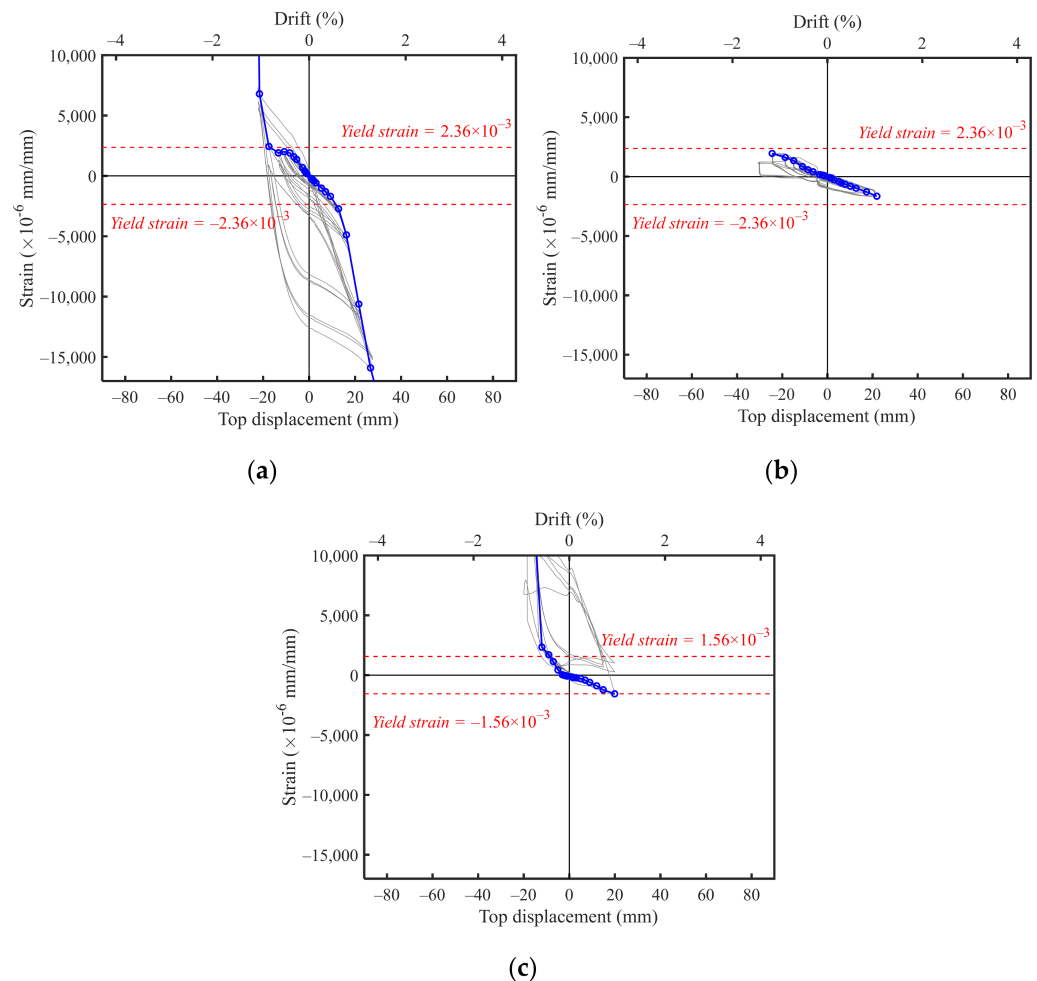


**Figure 18.** Strain response of vertical bars (No. 1 gauge in Figure 10). (a) W0; (b) W1-R; (c) W2-R.

The measured strains on the horizontal bars are depicted in Figure 19. Only the horizontal bar in W0 yielded slightly until the last load steps, while the bars in W1-R and W2-R were elastic during the test. This phenomenon indicates again that the shear force demand in PC walls was decreased by vertical connection, as mentioned in Section 3.2.

The strain of the vertical bar in W2-R upper wall part is also recorded, as depicted in Figure 20. The vertical bar yielded during the load step to 1.90% drift ratio (top displacement 40 mm), which was later than VT and earlier than VC. Though no horizontal strain gages were pasted on the upper wall parts, concerning the damage phenomenon, we could reconfirm that the failure mode of wall W2-R was a mixed mode of shear and flexure in the upper wall part.

The measured results of strain gages along the height of the end column are reported in Figure 21. In general, due to the flexure and vertical connection, the strain decreased with increasing height. Because the global deformation of the PC shear wall was dominated by wall panel, the strain of the end column increased rapidly once the plastic hinge region of wall panel occurred. As the test continued, the bottom of the end column yielded as the drift ratio reached 1.67% (top displacement 35 mm). As expected, strain increased faster once VT occurred, which means that VT would enlarge the axial force of the end column. The vertical bearing and associated axial force of the end column provided additional resistance moment for the shear walls.

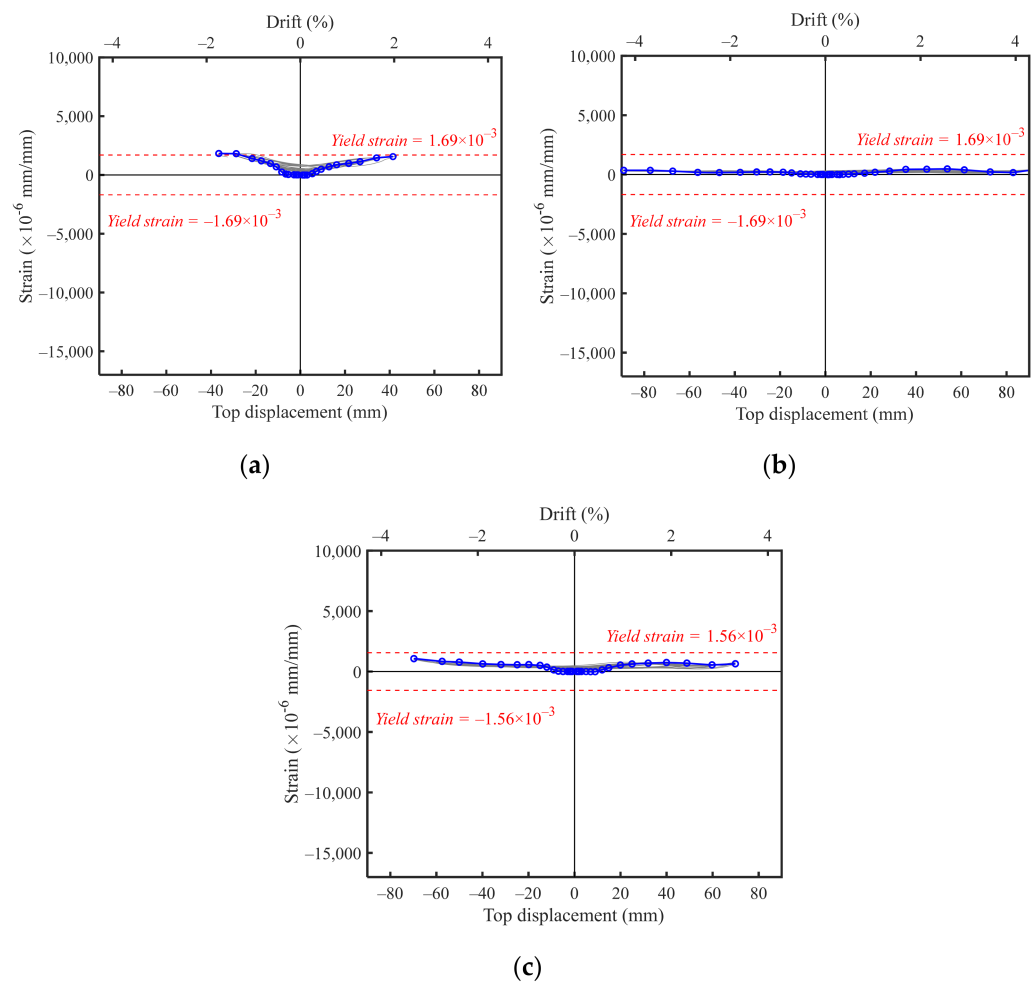


**Figure 19.** Strain response of horizontal bars. (a) W0 (No. 2 gauge in Figure 10); (b) W1-R (No. 2 gauge in Figure 10); (c) W2-R (No. 3 gauge in Figure 10).

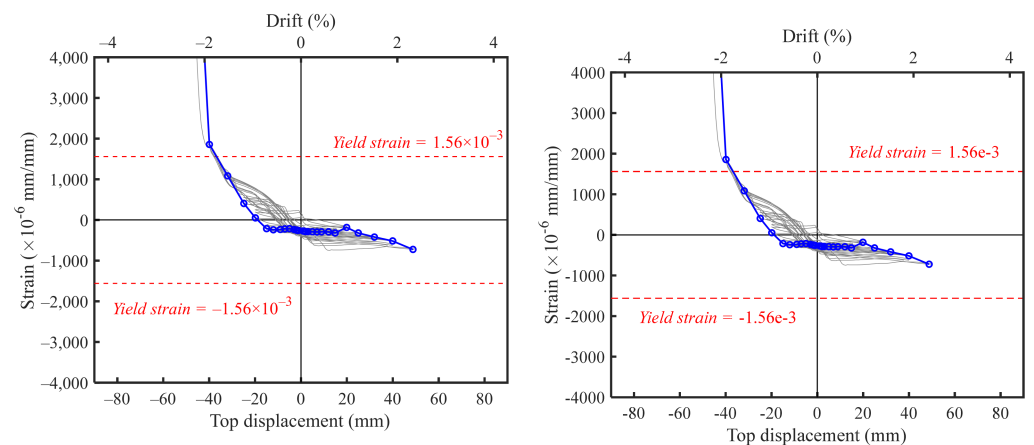


**Figure 20.** Strain response of vertical bars for upper wall part of W2-R (No. 4 gauge in Figure 10).

### 3.5. Stiffness Reduction and Energy Dissipation

Secant stiffness and energy dissipation are frequently used parameters to evaluate the seismic behaviour of PC members. The secant stiffness is defined as the slope of line which links the maximum loads of first cycle at positive and negative loading directions. The accumulated enclosed area of each hysteresis hoop is used to assess energy dissipation ability in various loading stages. Both two criteria, varying with the drift ratio of the walls, are illustrated in Figure 22.

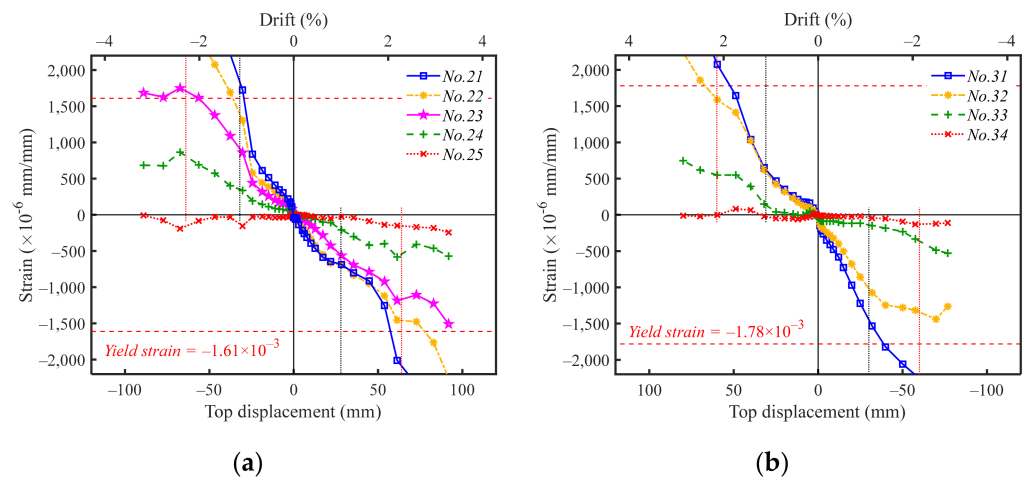


**Figure 21.** Comparison of strain results on end column. (a) W1-R; (b) W2-R.

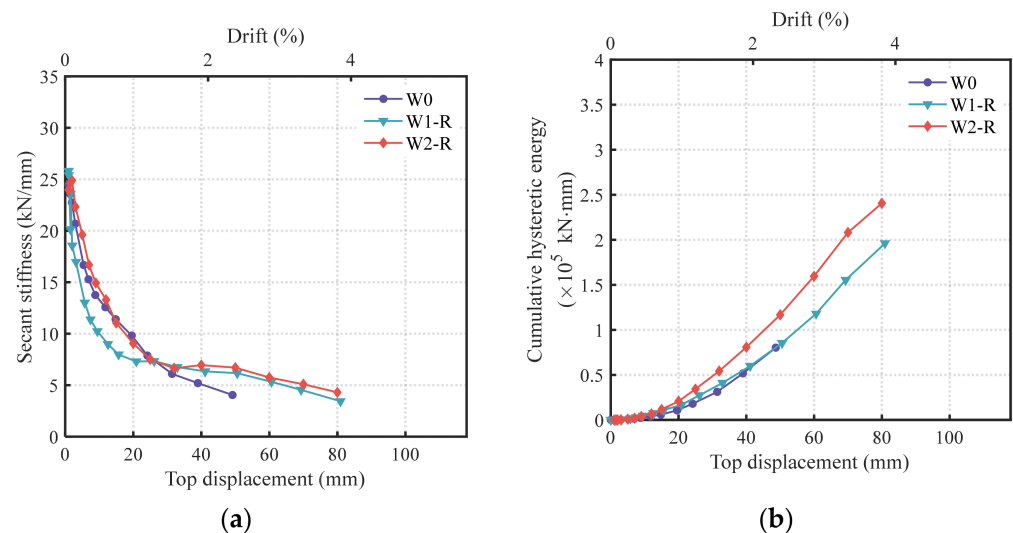


**Figure 22.** Comparison of stiffness degradation and cumulative energy dissipation. (a) Stiffness degradation; (b) Cumulative hysteretic energy.

Before VT occurred, the stiffness degradation of W0 and W2-R behaved comparably, but the curve of W1-R was lower. We inferred that more shrinkage cracks existed around the built-in bolt before loading, and that the weak vertical connection deteriorated the initial stiffness of W1-R. See Figure 22a, after the occurrence of VT, the tangent stiffness of two PC shear walls W1-R and W2-R were comparably flat, while the cast-in-place wall W0 kept falling. In detail, note that the curve of W2-R is slightly higher than W1-R after VT occurred, the reason is that strong vertical connection could provide stricter constraint; later VT brought additional stiffness and moment capacity and successfully delayed the degradation of the PC shear wall. Furthermore, VC had almost no obvious effect on the degradation.

Benefitting from the elevated drift capacities, both PC shear walls dissipated greater energy than W0 at the end of the test. The cumulative hysteretic energy of PC shear walls was increased by approximately two times compared with wall W0 at the end of the test. By comparing the cumulative hysteretic energy of walls, it was established that W2-R dissipated the most energy by benefitting a larger magnitude of friction in strong friction-bearing device.

#### 4. Discussion of Multiple Hardening

As described in previous sections, different failure modes were observed in PC walls. The secondary hardening phenomenon occurred in the PC wall with weak vertical connection (wall W1-R), concrete crushing around vertical connection and wall panel toes were found at the end of the test. The wall with strong vertical connection (wall W2-R) achieved the highest moment capacity and tertiary hardening. In this section, conceptual analysis of the multiple hardening phenomena is presented.

See Figure 23a, according to the Modified Compression Field Theory (MCFT) [31] and Rotating Angle Soften Truss Model (RA-STM) [32,33], the elongation enlarges the smeared tensile strain perpendicular to the crack direction with smeared diagonal cracks in the plastic hinge region. The effective compressive strength of concrete decreases as elongation increases, resulting in a reduction in the shear strength in plastic hinge. Most well-designed slender cast-in-place shear walls failed in a flexure or flexure-shear mode after flexural yielding, as depicted in Figure 23b. Different from the cast-in-place wall, PC walls in this study were equipped with vertical connection. Because of the elongation and associated VT, the elongation of the middle and bottom wall parts were restrained, see Figure 23c,d. Hence, flexural/shear strength of bottom/middle wall parts were enhanced, while the upper wall part was not.

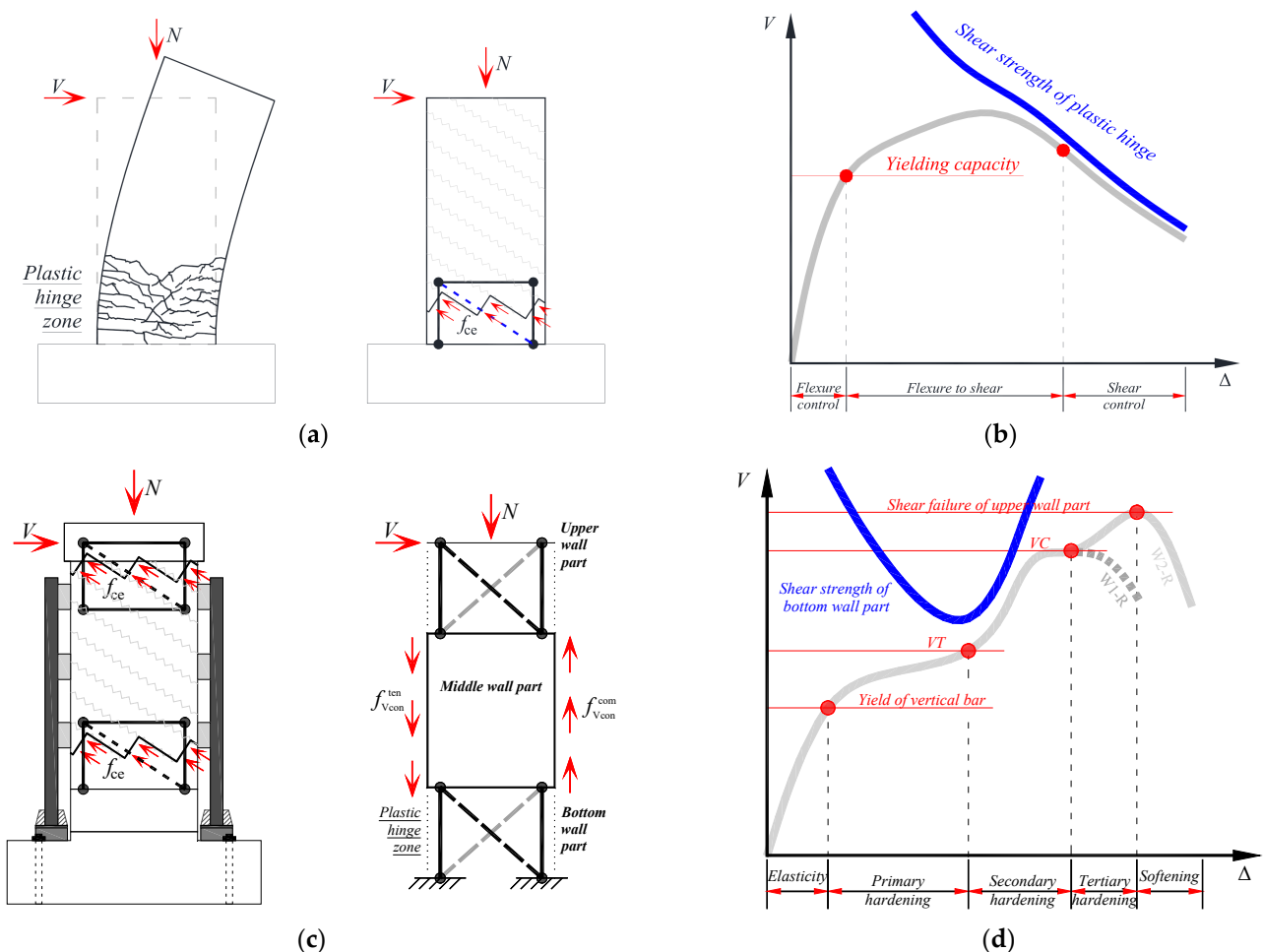


**Figure 23.** Conceptual analysis shear walls. (a) Load path and truss mechanism of slender cast-in-place wall; (b) Schematic of load–displacement relationship of slender wall [32,33]; (c) Load path and truss mechanism of PC wall; (d) Schematic of load–displacement relationship of PC wall.

Following above logic, for PC wall W1-R, the time of VT was consistent with the time when the concrete around the vertical connection began to crack, and the backbone curve

showed “secondary hardening”; however, the vertical connection was too weak to provide subsequent additional resistance moment, the time of the failure of vertical connection was consistent with VC, and later lateral load declined. For another PC wall W2-R, whose vertical connection was strengthened, the VT also caused the backbone curve to have “secondary hardening”. However, with strong vertical connection, the moment capacity of W2-R was re-elevated by VC, and “tertiary hardening” occurred gradually. Therefore, the failure model of W1-R was defined as a connection failure, while the one of W2-R was defined as shear failure at the upper wall part.

Predictably, as the limited slippage lengthens, shear strength of the plastic hinge region may drop quickly. Thus, for the PC wall with long limited slippage vertical connection, shear failure in the plastic hinge region may occur earlier than vertical bearing. In the existing parallel studies [22,34,35], PC shear walls with long limited slippage (22 mm) failed with web crushing of the bottom wall panel, which re-proved the validity of the conceptual analysis in this chapter; the photo is shown in Figure 24.



**Figure 24.** Web crushing failure of PC wall with long limited slippage vertical connection (blue and red lines represent the cracks as subjecting to different loading direction) [22,34,35].

## 5. Conclusions

An experimental programme consisting of quasi-static cyclic loading on shear walls was conducted. Two PC shear walls were designed with both horizontal and vertical connections. In the vertical connection, the friction-bearing devices and the end columns were used to assemble PC wall panels. The cyclic responses of PC shear walls with varying types of friction-bearing devices, namely weak connection and strong connection, were systematically investigated. The following conclusions can be summarized according to the current study.

- (1) The proposed PC shear walls first achieved “Vertical bearing of Tensile side” (“VT” for short), and then achieved “Vertical bearing of Compressive side” (“VC” for short). Once VT occurred, strong vertical connection almost stopped the vertical connection from slipping, while weak vertical connection did not.
- (2) The PC shear walls cracked slower than cast-in-place walls. Eventually, different failure modes were observed on three walls: W0 (cast-in-place wall) failed in flexure; W1-R (PC shear wall with weak vertical connection) failed with concrete crushing occurring around the friction-bearing devices and toes of the PC wall panels; and W2-R (PC shear wall with strong vertical connection) prevented the failure mode like W1-R, and later failed in a mixed mode of shear and flexure at the upper wall part.
- (3) The VT delayed the stiffness degradation of PC shear walls, thus leading to additional drift capacity and moment capacity. For wall W1-R, the time of VT was consistent with the time when the backbone curve achieved “secondary hardening”; the time of VC was consistent with the failure of vertical connection. For wall W2-R, benefitting

from the strengthened vertical connection, the wall also achieved “tertiary hardening”. In detail, the moment capacity of PC shear walls was increased by more than 60% when compared with the testing cast-in-place W0. The moment capacity of wall W2-R was higher than wall W1-R.

- (4) The magnitude of friction in the devices had a great influence on the energy dissipation, but not on the stiffness reduction and elongation. The cumulative hysteretic energy of the PC shear wall was increased by approximately two times compared with the cast-in-place W0.

**Author Contributions:** Conceptualization, H.J., J.S. and H.Q.; methodology, H.J. and J.S.; software, H.J. and H.C.; validation, H.J., Q.F. and D.C.; formal analysis, H.J. and W.G.; investigation, H.J. and Q.F.; data curation, H.J.; writing—original draft preparation, H.J.; writing—review and editing, H.J., H.C., W.G. and K.C.; visualization, H.C. and K.C.; supervision, H.Q. and D.C.; project administration, J.S. and H.J.; funding acquisition, J.S. and H.J. All authors have read and agreed to the published version of the manuscript.

**Funding:** This research was funded by the Lvyangjinfeng Talent Program of Yangzhou (Grant No. YZ-LYJFJH2021YXBS110); the Deputy Manager of Science and Technology Program of Jiangsu Province (Grant No. FZ20211212); the High-Level Talents Support Program of Yangzhou University (No. 137012283); Jiangsu Provincial Double-Innovation Doctor Program; the Natural Science Foundation of Jiangsu Province (Grant No. BK20170668).

**Institutional Review Board Statement:** Not applicable.

**Informed Consent Statement:** Not applicable.

**Data Availability Statement:** Correspondence and requests for materials should be addressed to H.J.

**Conflicts of Interest:** The authors declare no conflict of interest.

## References

- Carrillo, J.; Vargas, D.; Sánchez, M. Stiffness degradation model of thin and lightly reinforced concrete walls for housing. *Eng. Struct.* **2018**, *168*, 179–190. [CrossRef]
- Kurama, Y.C.; Sriharan, S.; Fleischman, R.B.; Restrepo, J.I.; Henry, R.S.; Cleland, N.M.; Ghosh, S.K.; Bonelli, P. Seismic-Resistant Precast Concrete Structures: State of the Art. *J. Struct. Eng.* **2018**, *144*, 03118001. [CrossRef]
- Clarivate Analytics. Web of Science. Available online: <https://www.webofscience.com> (accessed on 1 May 2022).
- Dang, L.J.; Liang, S.T.; Zhu, X.J.; Zhang, M.; Song, Y.M. Seismic performance of precast concrete wall with vertical energy-dissipating connection. *Struct. Des. Tall Spec.* **2021**, *30*, e1820. [CrossRef]
- Wu, D.; Liang, S.; Shen, M.; Guo, Z.; Zhu, X.; Sun, C. Experimental estimation of seismic properties of new precast shear wall spatial structure model. *Eng. Struct.* **2019**, *183*, 319–339. [CrossRef]
- Yan, J.-B.; Yan, Y.-Y.; Wang, T. Cyclic tests on novel steel-concrete-steel sandwich shear walls with boundary CFST columns. *J. Constr. Steel Res.* **2020**, *164*, 105760. [CrossRef]
- JGJ 1-2014; Technical Specification for Precast Concrete Structures. China Architecture & Building Press: Beijing, China, 2014.
- GB/T 51231-2016; Technical Standard for Assembled Buildings with Concrete Structure. China Architecture & Building Press: Beijing, China, 2017.
- Shen, S.-D.; Cui, Y.; Pan, P.; Gong, R.-H.; Miao, Q.-S.; Li, W.-F. Experimental Study of RC Prefabricated Shear Walls with Shear Keys Affected by a Slotted Floor Slab. *J. Aerosp. Eng.* **2019**, *32*, 04019013. [CrossRef]
- Wang, Y.L.; Zhang, Y.M.; Cui, H.J.; Cai, Z.J.; Xu, L.X. Experimental study on fabricated shear wall structure with energy-dissipating vertical joint. *Struct. Concr.* **2020**, *21*, 2654–2668. [CrossRef]
- Zhang, H.; Li, H.N.; Chen, X.Y.; Li, C. Experimental investigation on the hysteretic behavior of precast concrete walls with energy-dissipated dry connections. *Struct. Concr.* **2020**, *21*, 2836–2853. [CrossRef]
- Li, X.H.; Wu, G.; Kurama, Y.C.; Cui, H.R. Experimental comparisons of repairable precast concrete shear walls with a monolithic cast-in-place wall. *Eng. Struct.* **2020**, *216*, 110671. [CrossRef]
- Xu, L.H.; Xiao, S.J.; Li, Z.X. Behaviors and Modeling of New Self-Centering RC Wall with Improved Disc Spring Devices. *J. Eng. Mech.* **2020**, *146*, 04020102. [CrossRef]
- Han, Q.H.; Wang, D.Y.; Zhang, Y.S.; Tao, W.J.; Zhu, Y. Experimental investigation and simplified stiffness degradation model of concrete shear wall with steel connectors. *Eng. Struct.* **2020**, *220*, 110943. [CrossRef]
- Mangalathu, S.; Jang, H.; Hwang, S.-H.; Jeon, J.-S. Data-driven machine-learning-based seismic failure mode identification of reinforced concrete shear walls. *Eng. Struct.* **2020**, *208*, 110331. [CrossRef]

16. Eom, T.-S.; Park, H.-G.; Kim, J.-Y.; Lee, H.-S. Web Crushing and Deformation Capacity of Low-Rise Walls Subjected to Cyclic Loading. *ACI Struct. J.* **2013**, *110*, 575–584.
17. Paulay, T.; Priestley, M.J.N. Stability of ductile structural walls. *ACI Struct. J.* **1993**, *90*, 385–392.
18. Cheng, X.W.; Ji, X.D.; Henry, R.S.; Xu, M.C. Coupled axial tension-flexure behavior of slender reinforced concrete walls. *Eng. Struct.* **2019**, *188*, 261–276. [[CrossRef](#)]
19. Shegay, A.; Dashti, F.; Hogan, L.; Lu, Y.; Niroomandi, A.; Seifi, P.; Zhang, T.; Dhakal, R.; Elwood, K.; Henry, R.; et al. Research programme on seismic performance of reinforced concrete walls: Key recommendations. *Bull. N. Z. Soc. Earthq.* **2020**, *53*, 54–69. [[CrossRef](#)]
20. Masoudi, M.; Khajevand, S. Revisiting flexural overstrength in RC beam-and-slab floor systems for seismic design and evaluation. *Bull. Earthq. Eng.* **2020**, *18*, 5309–5341. [[CrossRef](#)]
21. NZS 3101:2006; Concrete Structures Standard. Standards New Zealand: Wellington, New Zealand, 2017.
22. Jiang, H.; Qiu, H.; Sun, J.; Del Rey Castillo, E.; Ingham, J.M. Influence of friction-bearing devices on seismic behavior of PC shear walls with end columns. *Eng. Struct.* **2020**, *210*, 110293. [[CrossRef](#)]
23. Mehrabani, R.V.; Sigrist, V. Elongation of Reinforced Concrete Plastic Hinges Subjected to Reversed Cyclic Loading. *J. Struct. Eng.* **2015**, *141*, 04014188. [[CrossRef](#)]
24. Henry, R.S.; Dizhur, D.; Elwood, K.J.; Hare, J.; Brunson, D. Damage to concrete buildings with precast floors during the 2016 Kaikoura earthquake. *Bull. N. Z. Soc. Earthq. Eng.* **2017**, *50*, 174–186. [[CrossRef](#)]
25. Dashti, F.; Dhakal, R.P.; Pampanin, S. Out-of-Plane Response of In-Plane-Loaded Ductile Structural Walls: State-of-the-Art and Classification of the Observed Mechanisms. *J. Earthq. Eng.* **2020**, *26*, 1325–1346. [[CrossRef](#)]
26. GB 50010-2010; Code for Design of Concrete Structures. China Architecture & Building Press: Beijing, China, 2016.
27. GB/T 50081-2002; Standard for Test Method of Mechanical Properties on Ordinary Concrete. China Architecture & Building Press: Beijing, China, 2003.
28. GB/T 228.1-2010; Metallic Materials-Tensile Testing-Part 1: Method of Test at Room Temperature. Standards Press of China: Beijing, China, 2011.
29. GB/T 50152-2012; Standard for Test Method of Concrete Structures. China Architecture & Building Press: Beijing, China, 2012.
30. JGJ/T 101-2015; Specification for Seismic Test of Buildings. China Architecture & Building Press: Beijing, China, 2015.
31. Vecchio, F.J.; Collins, M.P. The modified compression-field theory for reinforced concrete elements subjected to shear. *ACI J.* **1986**, *83*, 219–231.
32. Hsu, T.T.C. Softened truss model theory for shear and torsion. *ACI Struct. J.* **1988**, *85*, 624–635.
33. Lee, J.Y.; Watanabe, F. Shear deterioration of reinforced concrete beams subjected to reversed cyclic loading. *ACI Struct. J.* **2003**, *100*, 480–489.
34. Jiang, H. Behaviour of Precast Shear Wall with End Column Subjected to Seismic Loading. Ph.D. Thesis, Southeast University, Nanjing, China, 2020.
35. Fang, Q.; Qiu, H.X.; Sun, J.; Dal Lago, B.; Jiang, H.B. Performance study of precast reinforced concrete shear walls with steel columns containing friction-bearing devices. *Arch. Civ. Mech. Eng.* **2021**, *21*, 110. [[CrossRef](#)]